# Structural Characterization of Hellethionins from *Helleborus purpurascens*‡

Alexander G. Milbradt,§ Franz Kerek,|| Luis Moroder,§ and Christian Renner*,§

*Max-Planck-Institut für Biochemie and Donatur GmbH, 82152 Martinsried, Germany*

*Received October 14, 2002; Revised Manuscript Received January 2, 2003*

ABSTRACT: Thionins are relatively small-sized multiple-cystine peptides that are probably involved in the plant defense against pathogens. As such, these peptides constitute promising candidates for engineered plant resistance in the agricultural industry. More recently, thionins have been proposed as potential immunotoxins in tumor therapy. In the search for pharmacologically active natural products, a new family of thionins was recently discovered in the roots of *Helleborus purpurascens* that accordingly were termed hellethionins. The structural characterization by NMR of one representative member of this family, i.e., of hellethionin D, clearly reveals that thionins from different sources share a highly conserved overall fold. In fact, the well-defined 3D structure of hellethionin D is very similar to those reported so far for viscotoxins, purothionins, or crambin, although distinct differences could be detected in the C-terminal portion, especially for loop 36−39. These differences may derive from the unusual distribution of charged residues in the C-terminal half of the peptide sequence compared to other thionins and from the uncommon occurrence of four contiguous threonine residues in loop 36−39. As expected, reduction of the disulfide bonds in hellethionin D leads to complete unfolding, but upon oxidative refolding by air oxygen in the presence of glutathione the correct isomer is recovered in high yields, confirming the very robust fold of this class of bioactive cystine peptides.

Thionins are multiple-cystine peptides with a molar mass of about 5 kDa which play an important role in the defense mechanism of plants (*1*). Cereals (*Graminacea*) constitute a particularly rich source of thionins, e.g., purothionins were isolated from wheat (*Triticum aestivum*) (*2*), hordothionins from barley (*Hordeum vulgare*) (*3*), avenothionins from oats (*Avena sativa*) (*4*), and secalothionin from rye (*Secale cereale*) (*5*), and more recently thionins were found in cowpea (*Vigna unguiculata*) (*6*). Cereal thionins represent usual components of the food intake for humans and animals but are without significant oral toxicity due to their peptidic nature and thus facile enzymatic degradation. Other sources of thionins are parasitic plants such as mistletoe (*Viscum album*) for viscotoxins (*7*) and pyrularia nuts (*Pyrularia pubera*) for pyrularia thionin (*8*) as well as Abyssinnian cabbage (*Crambe abyssinica*) for crambin (*9*).

Thionins contain in their sequence six or eight cysteine residues involved in three or four disulfide bridges, respectively (*10*, *11*). Although the thionins known so far differ significantly in their sequence composition, the six cysteine residues at positions 3, 4, 16, 26, 32, and 40 as well as an arginine at position 10 and an aromatic residue at position 13 are well conserved. Almost all thionins are basic peptides, a fact that has been associated with their membrane activity. While the interaction with membrane phospholipids is essential for toxicity, it is not sufficient to cause cell lysis and death as well assessed with pyrularia thionin, which upon Trp-8 oxidation retains the identical membrane affinity but lacks hemolytic toxicity (*12*). Thionins are toxic to bacteria, fungi, and yeast in vitro, and this is assumed to reflect their possible role in the defense of plants against pathogens (*1*). Isolated viscotoxins A1 and A2 were found to induce apoptosis in cultured human lymphocytes, while in the case of the related viscotoxin B and pyrularia thionin this effect was not significant (*13*). The mechanism of the membrane activity of thionins is still under debate, but there is a good correlation between cytotoxicity and ability to form ion channels (*14*). The antimicrobial activity and cytotoxicity of thionins have led to the development of two potential applications: in agriculture transgenic plants containing thionin genes can enhance pathogen resistance (*15*), and targeting of thionins by tumor-specific antibodies is expected to support antitumor therapy (*16*).

For several thionins the three-dimensional (3D)[1] structure has been resolved by X-ray crystallography (*17*−*19*) and NMR (*20*, *21*). It resembles the Greek capital letter gamma (Γ) with the vertical stem represented by a pair of two antiparallel α-helices while the horizontal arm consists

‡ Coordinates of the NMR structure family of hellethionin D were deposited in the PDB database (http://www.rcsb.org/pdb, accession code 1NBL) together with the experimental NMR-derived NOE distance constraints. NMR assignments were submitted to the BMRB database (http://www.bmrb.wisc.edu/).

* Address correspondence to this author at Max-Planck-Institut für Biochemie, AG Bioorganische Chemie, Klopferspitz 18A, D-82152 Martinsried, Germany. Tel: 49-89-8578-3906. Fax: 49-89-8578-2847. E-mail: renner@biochem.mpg.de.

§ Max-Planck-Institut für Biochemie.

|| Donatur GmbH.

[1] Abbreviations: CD, circular dichroism; DQF-COSY, double-quantum-filtered correlated spectroscopy; 1D, one dimensional; 2D, two dimensional; 3D, three dimensional; DG, distance geometry; FID, free induction decay; *H. purpurascens*, *Helleborus purpurascens*; HPLC, high-pressure liquid chromatography; MD, molecular dynamics; NMR, nuclear magnetic resonance; NOE, nuclear Overhauser effect; NOESY, nuclear Overhauser and exchange spectroscopy; SA, simulated annealing; TOCSY, total correlation spectroscopy.

10.1021/bi020628h CCC: $25.00 
Published on Web 02/05/2003

of a short antiparallel double-stranded $\beta$-sheet. The ability of thionins to form membrane pores may be correlated to this structure where the charged polar groups are clustered on the inner bend between the helices and the $\beta$-sheet and are well separated from the more hydrophobic outer side of the $\Gamma$.

*Helleborus purpurascens* from the plant family of Ranunculaceae is a plant that was intensively used in ancient Greece to treat epilepsy and other psychic diseases. Its ethnobotanical use in the Balkan region was confirmed by a recent veterinarian study, which showed the efficacy by transcutaneous implantation of *H. purpurascens* roots in the treatment of chronic inflammatory diseases in pigs and sheep (*22*). From the same plant the cardiac glycoside hellebrin (*23*) with bufadienolidic structure (*24*) and other natural products (*25*) have been isolated in the past. More recently, novel substances belonging to macrocyclic carbon suboxide (MCS) derivatives were isolated from *H. purpurascens* (*26*) and characterized as highly potent inhibitors of Na,K-ATPase and of the SR Ca-ATPase (*27*). The search for additional bioactive compounds from the roots of this plant led to the identification and isolation of a new family of thionins (Kerek et al., manuscript in preparation).

In the present study the solution structure of one representative member of this class of thionins, isolated from the roots of *H. purpurascens*, was determined by NMR conformational analysis. The overall 3D structure is very similar to those reported for other thionins despite the significant sequence variations, thus confirming the robust scaffold character of the cystine network in this class of natural peptides.

## MATERIALS AND METHODS

*CD Measurements.* CD spectra were recorded on a JASCO J-715 spectropolarimeter equipped with a thermostated cell holder and connected to a data station for signal averaging and processing. All spectra were recorded in the wavelength range 190−250 nm employing quartz cuvettes of 0.1 cm optical path length. The average of 10 scans is reported and expressed in terms of ellipticity units per mole of peptide residues ($[\theta]_R$). Unless stated otherwise, all spectra were acquired at 25 °C and at peptide concentrations of 50 $\mu$M in water.

*NMR Measurements.* The hellethionin D samples for the 2D NMR spectroscopy contained 3−5 mM natural peptide at pH 2.5 in 0.5 mL of $H_2O/D_2O$ (9:1) or $D_2O$. NMR experiments for the determination of the spatial structure were performed at proton frequencies of 500 and 750 MHz on Bruker DRX500 and DMX750 spectrometers. Different temperatures (283, 293, and 303 K) were chosen to resolve signal overlap. Resonance assignment was performed with the program SPARKY (*28*) according to the method of Wüthrich (*29*). The 2D TOCSY spectra were recorded with spin-lock periods of 75 ms using the MLEV-17 sequence for isotropic mixing (*30*). Experimental interproton distance constraints were extracted from 2D NOESY experiments (*31*) with mixing times between 50 and 150 ms. NOE buildup curves of representative peaks indicated spin diffusion for longer mixing times. $^3J_{HN-HA}$ coupling constants were extracted from 2D DQF-COSY spectra (*32*). Temperature shift coefficients for the amide protons were obtained from TOCSY spectra recorded at 283, 293, and 303 K. Deuterium exchange rates were measured at 277 K after a lyophilized sample in $D_2O$ was dissolved on ice. Amide hydrogen bonds were identified according to two criteria: protection of the amide proton from H/D exchange and temperature shift coefficients less negative than $-5$ ppb $K^{-1}$. Water suppression was achieved either by using the WATERGATE sequence (*33*) or by presaturation. Translational diffusion constants were measured at 300 K with standard experiments provided with the NMR acquisition software XWINNMR (Bruker Biospin, Karlsruhe, Germany) using a diffusion delay of 200 ms. Diffusion constants were calibrated to a diffusion constant of $18.7 \times 10^{-10}$ $m^2$ $s^{-1}$ for $H_2O$ in $D_2O$ at 300 K. Data processing was performed using the XWINNMR software package on SGI Workstations.

Table 1: Statistics of the NMR Structure Ensemble

| | |
|---|---|
| distance constraints | 594 |
| intraresidual NOEs | 90 |
| sequential NOEs | 175 |
| medium-range NOEs | 160 |
| long-range NOEs | 152 |
| hydrogen bonds | 17 |
| RMSDs (Å) | |
| all backbone | 0.36 |
| all heavy | 0.62 |
| secondary structure elements, backbone | 0.25 |
| secondary structure elements, heavy | 0.70 |
| energy (kcal/mol) (mean ± SD) | |
| van der Waals energy | $-59.38 \pm 2.98$ |
| hydrogen bond energy | $-18.76 \pm 0.74$ |
| Coulomb energy | $53.28 \pm 3.69$ |
| Ramachandran plot | |
| most favored regions (%) | 80.7 |
| additional allowed regions (%) | 18.9 |
| generously allowed regions (%) | 0.3 |

*Structure Calculations.* Structure calculations and evaluations were performed with the INSIGHTII (Version 98) software package (Accelrys, San Diego) on Silicon Graphics O2 R5000 and Origin 200 computers. The NOE intensities were converted into interproton distance constraints using the following classification: very strong (vs), 1.7−2.3 Å; strong (s), 2.2−2.8 Å; medium (m), 2.6−3.4 Å; weak (w), 3.0−4.0 Å; and very weak (vw), 3.2−4.8 Å. The distances of pseudoatoms were corrected as described by Wüthrich (*29*). NOEs were not filtered for structural relevance. Hydrogen bonds were implemented as distance constraints with an upper limit of 2.5 Å between the amide proton and the carbonyl oxygen. Although qualitatively in agreement with the determined secondary structure, determination of $^3J_{HN-HA}$ coupling constants was not possible with sufficient accuracy for use in the structure calculation due to some aggregation tendency of hellethionin D at millimolar concentrations. The force constant used for the distance constraints and the hydrogen bonds was 50 kcal $mol^{-1}$ $Å^{-2}$, and constraints were applied at every stage of the calculations. One hundred structures were generated by distance geometry in four dimensions, then reduced to three dimensions with the EMBED algorithm (*34*), and optimized with a simulated annealing step (*35*), maintaining the distance constraints according to the standard protocol of the DG II package of INSIGHTII. Subsequently, the structures were refined with a MD−SA protocol: after an initial minimization of 1000 steps, 5 ps at 500 K was simulated followed by exponential cooling to ~0 K during 10 ps. The molecular dynamics simulations were all performed with the AMBER force field

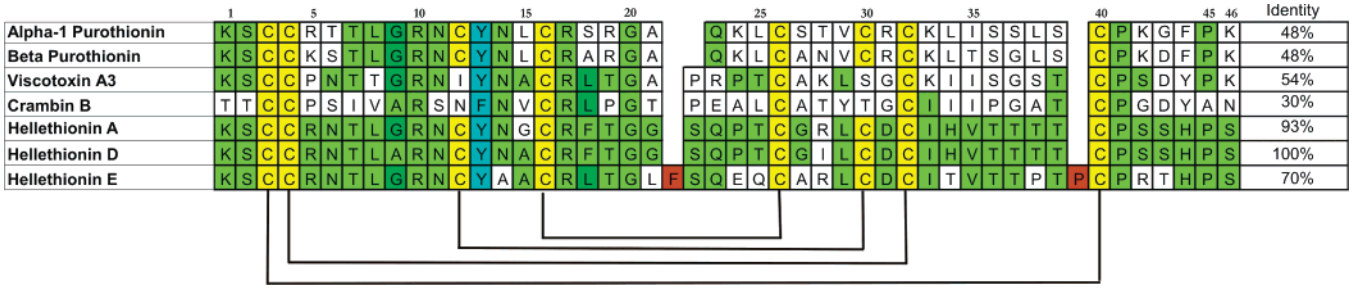


FIGURE 1: Sequence alignment of some of the recently discovered hellethionins (F. Kerek, manuscript in preparation) with other known type II $\gamma$-thionins. Color coding: green = sequence identity to hellethionin D, red = insertion, yellow = conserved disulfide pattern, and blue = highly functional relevant Tyr-13 (see text).

with 1 fs time steps. Of the 100 calculated structures, the 20 structures with lowest energy were selected for further characterization. In initial structure calculations no disulfide bonds were used as the disulfide bond pattern was unknown in the beginning. However, disulfide bonds were unambiguously defined by these initial calculations. For final structure calculations disulfide bridges were implemented as covalent bonds. Secondary structure elements were identified with the Kabsch−Sander algorithm as implemented in INSIGHTII. Ramachandran plots and RMSDs were calculated using PROCHECK (*36*) (Table 1). For the graphical presentation of the structures INSIGHTII and MOLMOL (*37*) were used.

*Oxidative Refolding of Hellethionin D.* Hellethionin D was reduced at 1 mM concentration in aqueous solution (500 $\mu$L) by addition of tris(2-carboxyethyl)phosphine (14 mmol). Progress of the reaction was monitored by $^1$H-1D NMR and was found to be complete after 24 h at 50 °C. CD spectra were recorded on diluted aliquots (50 $\mu$M peptide concentration) before and after unfolding. For refolding experiments the excess phosphine was removed by gel chromatography using a NAP-5 column (Pharmacia, Erlangen, Germany) and 50 mM Tris-HCl buffer (pH 7.2) as eluent. Refolding of the solution with ~0.5 mM reduced hellethionin D in 50 mM Tris-HCl buffer (pH 7.2) was allowed to proceed under air oxygen overnight at 37 °C. Alternatively, reoxidation was performed under identical conditions in the presence of glutathione at a GSSG:GSH:peptide ratio of 100:10:1. $^1$H-1D NMR spectra served to evaluate the yield of correctly refolded hellethionin D by comparison with spectra before (100% folded) and after reduction (100% unfolded). Additional quantification of the product distribution was achieved by RP-HPLC on a $C_{18}$ column (Machery & Nagel, Düren, Germany) eluting with a linear gradient of 2% $H_3PO_4$/acetonitrile from 5% to 80% acetonitrile in 15 min at a flow rate of 1.5 mL min$^{-1}$. Yields of correct oxidative refolding were extracted from the peak areas of the HPLC chromatograms.

## RESULTS

The new family of thionins isolated from *H. purpurascens* shows a highly conserved sequence composition (56%) but only 22% identity with the thionins from other plant sources (Figure 1). All contain eight cysteine residues at identical positions as the other thionins, and as expected, their connectivities are also identical as assessed by NMR conformational analysis of one representative member, i.e., hellethionin D. Compared to other thionins sequence differences

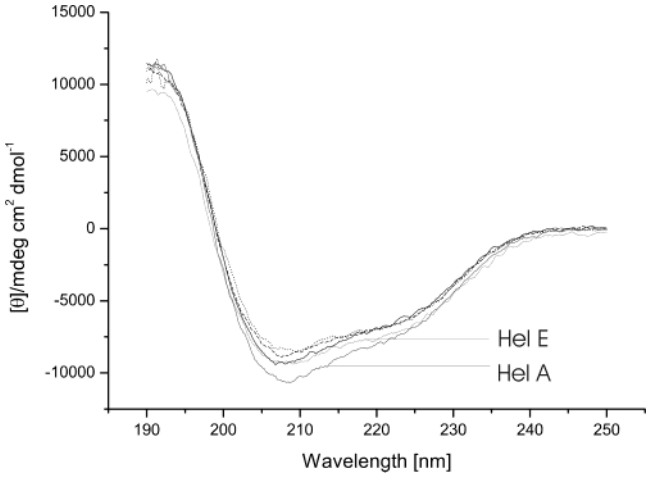


FIGURE 2: CD spectra of hellethionins. Spectra of hellethionin D at pH 2.6 (solid line), pH 4.2 (broken line), and pH 7.7 (dotted) are shown together with spectra from hellethionin A (Hel A) and hellethionin E (Hel E) at pH 7.

are mainly observed in the C-terminal part, and worthy to note is the cluster of contiguous threonine residues in the sequence portion 36−39.

### *Structural Analysis of Hellethionin D*

To investigate whether even the hellethionins retain the typical Γ fold of the thionins, a detailed structural analysis was carried out on one member of this new family, i.e., hellethionin D from *H. purpurascens*.

*CD Spectroscopy.* CD spectra in aqueous solution exhibit no pH dependence between pH 2.5 and pH 7.7 (Figure 2), indicating that no major structural changes occur in this pH range. The spectrum is typical of a mostly α-helical conformation in accordance with known thionin structures. The peptide fold is stabilized by four disulfide bonds and is therefore characterized by a high thermostability. In fact, thermal denaturation as monitored by CD spectra shows no appreciable unfolding up to 90 °C; CD spectra remain qualitatively the same with a slight reduction in intensity with increasing temperature. Figure 2 also includes CD spectra of hellethionin A and hellethionin E at pH 7, which are very similar to those of hellethionin D.

*NMR Assignment and Secondary Structure.* NMR experiments on hellethionin D were performed on natural peptide samples dissolved in deionized water at pH 2.5, which probably results from trifluoroacetic acid contamination of the HPLC-purified samples. The pH was not adjusted to higher values to exploit the slow proton exchange at low

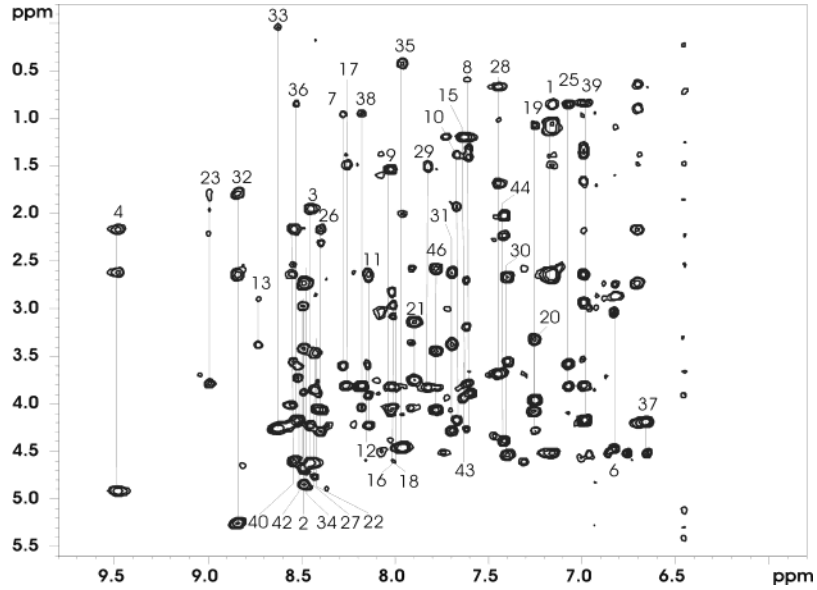


FIGURE 3: NMR fingerprint region HN−H (aliphatic) of the TOCSY spectrum of hellethionin D recorded at 750 MHz and 293 K with assignment (sequence numbers). The resonances of Arg-5 were not observed in the TOCSY spectrum.

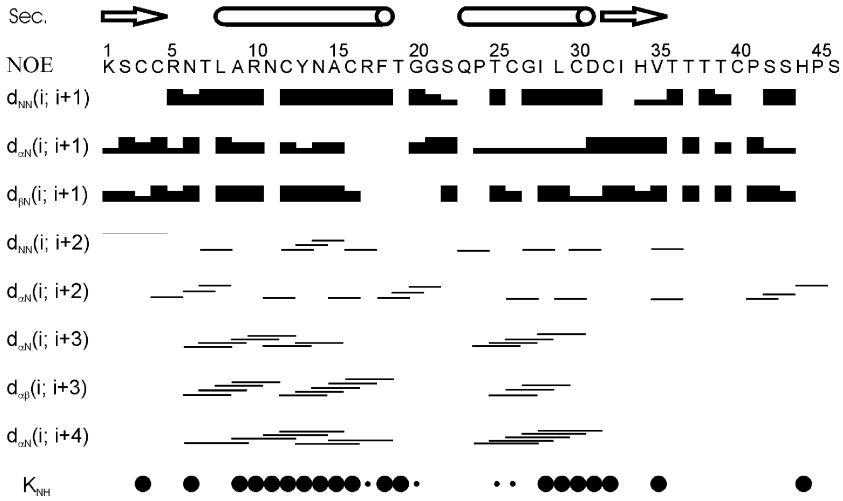


FIGURE 4: Secondary structure plot: Compilation of characteristic NOEs and H/D exchange of hellethionin D. Secondary structure elements are indicated above the sequence. In the last row small circles indicate moderately slow and large circles indicate slow amide−proton exchange.

pH values, since CD spectra confirmed full retention of the overall structure at pH 2.5 (Figure 2). The NMR spectra were of good quality, and unambiguous assignment was possible for all amino acids (Figure 3) except for the Hα of Thr-36, which is part of a loop sequence containing four sequential Thr residues. In Figure 4 characteristic NOEs defining secondary structure elements and H/D exchange are compiled. A long α-helix (α1 from Leu-8 to Phe-18) and a shorter α-helix (α2 from Pro-23 to Asp-31) are readily recognized. Additionally, two short $\beta$-strands, $\beta$1 (Lys-1 to Cys-4) and $\beta$2 (Asp-32 to His-35), form a short antiparallel $\beta$-sheet. Thus, as observed for other thionins, hellethionin D displays the typical $\beta\alpha\alpha\beta$ motif.

*Oligomeric State of Hellethionin D in Water*. To ensure that in our NMR samples hellethionin D is present in monomeric form, we performed dilution and NMR diffusion experiments. A slight line narrowing is observed upon dilution from 4 to 2 mM, but no further line narrowing is seen when diluting to 0.1 mM peptide concentration. Translational diffusion constants determined by NMR in water at 300 K were $1.4 \times 10^{-10}$ m$^2$ s$^{-1}$ at all concentrations. This diffusion constant is typical for a 5 kDa compact protein and confirms that hellethionin is present in solution mostly as monomer. The limited line broadening at high concentrations probably reflects a moderate tendency for unspecific aggregation of hellethionin D.

*3D Solution Structure.* The three-dimensional structure of hellethionin D in solution is well defined by 577 NOE distance constraints and 17 hydrogen bonds. The observed NOEs are rather equally distributed over the sequence (Figure 5) as typical for a compact fold. In addition to the NOEs defining α-helices and $\beta$-sheet, many interresidual NOEs connecting different parts of the polypeptide sequence were observed, leading to mostly well-defined loops between secondary structure elements. The pattern of the disulfide bonds was not known a priori but resulted unequivocally from initial structure calculations without disulfide bonds. The Cys-3 and Cys-4 residues at the N-terminus are linked to Cys-40 and Cys-32, respectively. Cys-12 is disulfide bonded to Cys-30, while Cys-16 and Cys-26 form the fourth

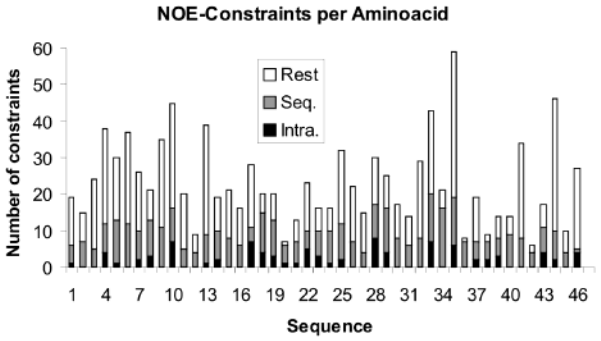


FIGURE 5: Number of NOE constraints per residue for each amino acid: black = intraresidual, gray = sequential, and colorless = medium- and long-range NOEs.

disulfide bridge, in full agreement with the disulfide connectivities of other thionins with four disulfide bonds. As a natural product preparation was used for the study, the cysteine connectivities correspond to the native disulfide pattern.

Figure 6 displays a stereoview of the 20 lowest energy structures superimposed on the backbone. From this structure it is evident that hellethionin D belongs to the group of $\gamma$-thionins that are characterized by a global fold reminiscent of the Greek letter Γ. The ribbon drawing of hellethionin D in Figure 7 visualizes how the long arm of the Γ (upside down) is composed of the two antiparallel α-helices whereas the $\beta$-sheet constitutes the short arm. Of the four disulfide bonds, two are buried in hydrophobic cores, while the Cys-3/Cys-40 and the Cys-16/Cys-26 disulfide are more exposed to the bulk solvent. Additionally, the side chains of residues 13, 23, and 33 that have been proposed to be involved in the biological activity (*21*) are highlighted. Very important seems to be the highly conserved Tyr-13 as iodination of this side chain leads to loss of toxicity in mice and yeast (*38*). The RMSD for backbone atoms of all amino acids is 0.36 Å; for heavy atoms it is 0.62 Å. Remarkable and in contrast to known thionin structures is the highly defined C-terminal sequence that is stabilized in hellethionin D by a hydrogen bond between the C-terminal Ser-46 and Cys-4. Regions of highest disorder are loop Thr-19 to Gln-23 between helices α1 and α2 and loop Thr-36 to Thr-39 (Figure 8). While the NMR structure family exhibits a less defined conformation for loop Thr-36 to Thr-39, indicating some flexibility in this region, the Thr-19 to Gln-23 loop exists in multiple conformations (Figure 6). The major conformation (12 out of the 20 lowest energy structures) is well defined, but minor conformations are observed that are rather different in the backbone arrangement, and these are responsible for the high RMSD observed for this portion of the molecule (Figure 8). For Ser-22 an additional set of resonance frequencies was present in the spectra, indicating that conversion between conformers is slow.

### *Oxidative Refolding of Hellethionin D*

Reductive unfolding and oxidative refolding experiments were performed to possibly identify the main factors that affect the stability of the hellethionin D structure and to analyze the intrinsic propensity of the hellethionin D for correct oxidative refolding. Reduction of the disulfide bonds with excesses of tris(2-carboxyethyl)phosphine in acidic aqueous solution was found to proceed at slow rate as monitored by $^1$H NMR. Quantitative reduction was achieved upon incubation at 50 °C for 24 h, and both the $^1$H NMR spectra and CD spectra confirmed the complete loss of ordered structure within the detection limits. It is well established that oxidative refolding of multiple-cystine peptides even of lower masses, e.g., bee or snake venom toxins (*39*) and conotoxins (*40*), regenerates under more or less optimal conditions the correctly folded isomers often in very high yields. Although these molecules are all products of enzymatic processing of the folded propeptides, sufficient information is apparently encoded in the sequence for correct refolding. Thereby, burying of the disulfides into hydrophobic cores of globular structures was suggested as the main driving force (*41*). Also thionins are processed from pro forms (*1*); nevertheless, air oxidation of the fully reduced hellethionin D at pH 7.2 and in a more efficient manner in the presence of glutathione, which drives the product distribution to the thermodynamically most favored structure, leads to high recoveries of the correct isomer (50% in the case of air oxidation and almost 100% in the presence of GSSG/GSH). Again, the sequence-encoded information drives the thermodynamically coupled oxidative refolding

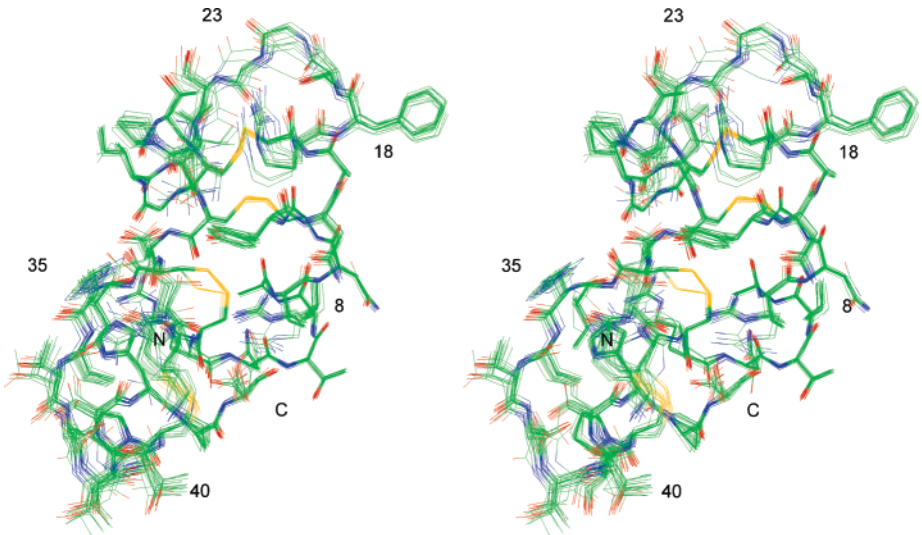


FIGURE 6: Stereoview of the NMR-derived structure family (20 lowest energy) of hellethionin D. Atoms are colored according to atom type; only heavy atoms are displayed.

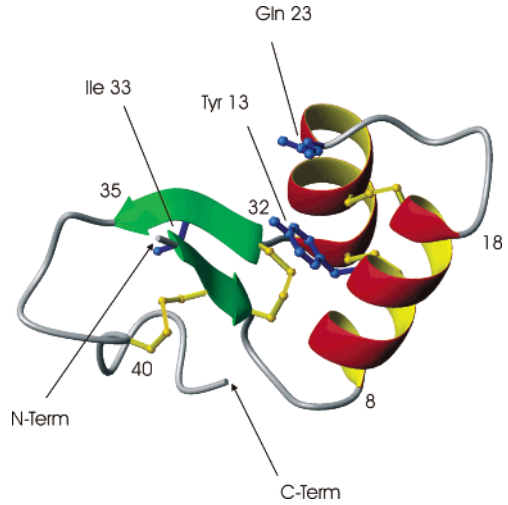


FIGURE 7: Ribbon drawing of the NMR solution structure of hellethionin D. Side chains of amino acids that have been proposed for biological activity (*21*) are highlighted in blue, and disulfide bonds are displayed in yellow.

process to the native hellethionin D structure as well assessed by comparing the CD and $^1$H NMR spectra of native and refolded hellethionin D.

## DISCUSSION

For a comparison of the spatial structure of hellethionin D with those previously reported for other thionins (*21*, *18*, *19*), the backbone of hellethionin D was superimposed to that of viscotoxin A3 (*21*), $\beta$-purothionin (*18*), and crambin (*19*) (Figure 9). The α-helices and $\beta$-sheet compare very well with backbone RMSDs for secondary structure elements of 0.7 Å to viscotoxin, 0.9 Å to purothionin, and 0.92 Å to crambin. Some spread out of conformations is observed for residues 19−21 of the loop between helix α1 and helix α2. More prominent are differences observed for hellethionin D in the C-terminal part following $\beta$-strand $\beta$2. Purothionin, crambin, and viscotoxin share a very similar arrangement of turns and bends for the last 12 amino acids, whereas hellethionin D is rather dissimilar from other thionins from residue Thr-36 vs the C-terminus. Only the C-terminus itself comes again close to the C-termini of the other $\gamma$-thionins. Obviously, differences are limited by the presence of the conserved disulfide bridge between Cys-3 and Cys-40. Although the structure ensemble of hellethionin D is less defined for residues Thr-36 to Thr-39 (Figure 8), the spread out of conformations is small compared to the difference regarding the loop conformation displayed by the other thionins; this would mean that the difference is not caused by lack of experimental data for this loop of hellethionin D. This view is supported by numerous medium- and long-range NOEs that are observed for the C-terminal residues. Finally, if in hellethionin D the 36−39 loop would exist in a conformation similar to that of the other thionins, the backbone atoms of Thr-37 and Thr-38 would be very close to the side chain amino group of Lys-1. However, NOEs between these atoms can definitely be excluded in the NOESY spectra. Although the significance as well as the origin of the difference between hellethionin D and other thionins in the C-terminal conformation and especially in loop Thr-36 to Thr-39 is unknown at the moment, it can be speculated that these arise from the different charge distribution (vide infra) and the Thr-rich 36−39 region present in hellethionin D.

At pH 7.0 hellethionin D is positively charged. In the N-terminal half of the sequence the pattern of charged amino acids present in hellethionins (Lys-1, Arg-5, Arg-10, and Arg-17) is identical as in other thionins. However, large differences exist in the second part of the molecule (Figure 1). The positive charges found in other thionins are not present in hellethionin D. The side chains of Asp-31 and Arg-5 are in spatial proximity (Figure 6) and probably form a salt bridge at physiological pH.

In summary, hellethionin D as representative of a larger new family of thionins was found to exhibit the typical thionin structure with a pattern of disulfide bridges, which corresponds to that of type II $\gamma$-thionins (*1*). Despite this common fold, significant differences are observed in the C-terminal part between other $\gamma$-thionins and the newly discovered hellethionins, which are probably caused by the unusual charge distribution and the threonine-rich sequence portion 36−39. Whether the diversity in sequence composition of the thionins with the associated local structural differences reflects evolution-driven optimized biological functions in the different plant sources has to be established. For this purpose the high propensity of hellethionin D to refold correctly into the native structure, a property probably shared by all thionins because of the common structural motif and disulfide pattern, makes these molecules robust scaffolds that can be exploited for expression of libraries of molecules mutated in defined sequence positions for screening of optimized membrane activities and cytotoxicity. A similar

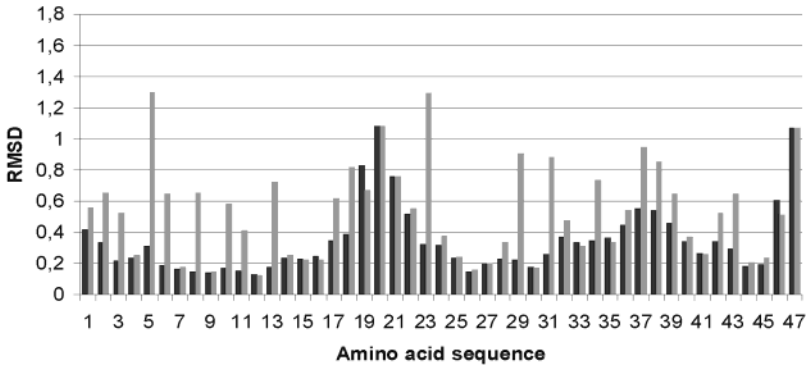


FIGURE 8: RMSD of 20 lowest energy structures of hellethionin D per residue. Black bars correspond to RMSD of backbone heavy atoms and gray bars to RMSD of all heavy atoms including side chains.

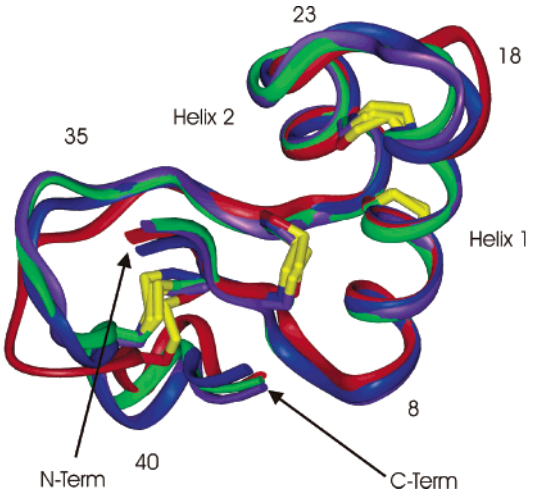


FIGURE 9: Superimposition of backbone atoms in secondary structure elements of hellethionin D (red ribbon) with viscotoxin A3 (blue, PDB code 1EDO) (*20*), $\beta$-purothionin (green, PDB code 1BHP) (*17*), and crambin (violet, PDB code 1EJG) (*19*).

approach has recently been applied to libraries of low mass multiple-cystine peptides (*42*, *43*).

## ACKNOWLEDGMENT

The skillful technical assistance of Mrs. Elisabeth Weyher in spectroscopy is gratefully acknowledged.

## REFERENCES

1. Garcia-Olmedo, F., Molina, A., Alamillo, J. M., and Rodriquez-Palenzuela, P. (1998) Plant defense peptides, *Biopolymers 47*, 479−491.
2. Balls, A. K., Hale, W. S., and Harris, T. H. (1942) A crystalline protein obtained from liopoprotein of wheat flour, *Cereal Chem. 19*, 279−288.
3. Redman D. G., and Fisher, N. (1969) Purothionin analogues from barley flour, *J. Sci. Food Agric. 19*, 651−655.
4. Békés, F., and Lasztity, R. (1981) Isolation and determination of amino acid sequence of avenothionin, a new purothionin analogue from oat, *Cereal Chem. 58*, 360−361.
5. Hernandez-Lucas, C., Carbonero, P., and Garcia-Olmedo, F. (1978) Identification and purification of a purothionin homologue from rye (*Secale cereale* L.), *J. Agr. Food Chem. 25*, 794−796.
6. Melo, F. R., Ridgen, D. J., Franco, O. L., Mello, L. V., Ary, M. B., Grossi de Sa, M. F., and Bloch, C. (2002) Inhibition of trypsin by cowpea thionin: Characterization, molecular modeling, and docking, *Proteins 48*, 311−319.
7. Schaller, G., Urech, K., and Giannattasio, M. (1996) Cytotoxicity of different viscotoxins and extracts from the european subspecies of *Viscum Album* L, *Phytother. Res. 10*, 473−477.
8. Vernon, L. P., Evett, G. E., Zeikus R. D., and Gray, W. R. (1985) A toxic thionin from Pyrularia pubera: purification, properties, and amino acid sequence, *Arch. Biochem. Biophys. 238*, 18−29.
9. Teeter, M. M., Mazer J. A., and L'Italien, J. J. (1981) Primary structure of the hydrophobic plant protein crambin, *Biochemistry 20*, 5437−5443.
10. Florack, D. E. A., and Stiekema, W. J. (1994) Thionins: properties, possible biological roles and mechanisms of action, *Plant Mol. Biol. 26*, 25−37.
11. Bohlmann, H., and Apel, K. (1991) Thionins, *Annu. Rev. Plant Physiol. Plant Mol. Biol. 42*, 227−240.
12. Fracki, W. S., Li, D., Owen, N., Perry, C., Naisbitt, G. H., and Vernon, L. P. (1992) Role of Tyr and Trp in membrane responses of pyrularia thionin determined by optical and NMR Spectra following Tyr iodination and Trp modification, *Toxicon 30*, 1427−1440.
13. Büssing, A., Stein, G. M., Wagner, B., Schaller, G., Pfüller, U., and Schietzel, M. (1999) Accidental cell death and generation of reactive oxygen intermediates in human lymphocytes induced by thionins from *Viscum album*, *Eur. J. Biochem. 262*, 79−87.
14. Hughes, P., Dennis, E., Whiteross, M., Llewellyn, D., and Gage, P. (2000) The cytotoxic plant protein, $\beta$-purothionin, forms ion channels in lipid membranes, *J. Biol. Chem. 275*, 823−827.
15. Ohashi, Y., Mitsuhara, I., Oshshima, M., Ugaki, M., Hirochika, H., Honkura, R., Iwai, T., and Nakamura, S. (1998) U.S. Patent 6,187,995.
16. Gasanov, S. E., Rael, E. D., Gasanov, N. E., and Vernon, L. P. (1995) In vitro evaluation of *Pyrularia* thionin-anti-CD5 immunotoxin, *Cancer Immunol. Immunother. 43*, 122−128.
17. Stec, B., Rao, U., and Teeter, M. M. (1995) Refinement of purothionins reveals solute particles important for lattice formation and toxicity, Part 1. $\alpha$-1-Purothionin revisited, *Acta Crystallogr., Sect. D 51*, 914−924.
18. Stec, B., Rao, U., and Teeter, M. M. (1995) Refinement of Purothionins Reveals Solute Particles Important for Lattice Formation and Toxicity, Part 2: Structure of Beta-Purothionin at 1.7 Angstroms Resolution, *Acta Crystallogr., Sect. D 51*, 914−924.
19. Jelsch, C., Teeter, M. M., Lamzin, V., Pichon-Lesme, V., Blessing, B., and Lecomte, C. (2000) Accurate protein crystallography at ultra-high resolution: valence-electron distribution in crambin, *Proc. Natl. Acad. Sci. U.S.A. 97*, 3171−3176.
20. Clore, G. M., Nilges, M., Sukumaran, K. D., Bruenger, A. T., Karplus, M., and Gronenborn, A. M. (1986) The three-dimensional structure of $\alpha$1-purothionin in solution: combined use of nuclear magnetic resonance, distance geometry and restrained molecular dynamics, *EMBO J. 5*, 2729−2735.
21. Romagnoli, S., Ugolini, R., Fogolari, F., Schaller, G., Urech, K., Giannattasio, M., Ragona, L., and Molinari, H. (2000) NMR structural determination of viscotoxin A3 from *Viscum album* L., *Biochem. J. 350*, 569−577.
22. Bogdan, I., Nechifor, A., Basea, I., and Hruban, E. (1997) From Rumanian folk medicine: nonspecific stimulus therapy using transcutaneous implantation of hellebore (*Helleborus purpurascens*, Fam. Ranunculaceae) in agriculturally useful animals, *Dtsch. Tieraerztl. Wochenschr. 97*, 525−529.
23. Cioaca C., and Cucu, V. (1974) Quantitative determination of hellebrin in the rhizomes and roots of *Helleborus purpurascens* W. et K., *Planta Med. 26*, 250−253.
24. Muhr, P., Kerek, F., Dreveny, D., Likussar. W., and Schubert-Zsilavecz, M. (1995) The structure of hellebrin, *Liebigs Ann. Chem. 1994*, 443−444.
25. Kissmer, B., and Wichtl, M. (1987) Ecdysone from roots and seeds of *Helleborus* species, *Arch. Pharmacol. 320*, 541−546.
26. Kerek, F. (2000) The structure of the digitalis like and natriuretic factors identified as macrocyclic derivatives of the inorganic carbon suboxide, *Hypertens. Res. 23*, 33−38.
27. Kerek, F., Stimac, R., Apell, H.-J., Freudenmann, F., and Moroder, L. (2002) Characterization of the macrocyclic carbon suboxide factors as potent Na,K-ATPase and SR Ca-ATPase inhibitors, *Biochim. Biophys. Acta 1567*, 213−220.
28. Goddard, K., and Kneller, D. G. Sparky 3, University of California, San Francisco.
29. Wüthrich, K. (1986) *NMR of Proteins and Nucleic Acids*, John Wiley, New York.
30. Bax, A., and Davis, D. G. (1985) MLEV-17-based two-dimensional homonuclear magnetization transfer spectroscopy, *J. Magn. Reson. 65*, 355−360.
31. Jeener, J., Meier, B. H., Bachman, P., and Ernst, R. R. (1979) Investigation of exchange processes by two-dimensional NMR spectroscopy, *J. Chem. Phys. 71*, 4546−4553.
32. Rance, M., Sorensen, O. W., Bodenhausen, G., Wagner, G., Ernst, R. R., and Wüthrich, K. (1983) Improved spectral resolution in cosy 1H NMR spectra of proteins via double quantum filtering, *Biochem. Biophys. Res. Commun. 117*, 479−485.
33. Sklenar, V., Piotto, M., Leppik, R., and Saudek, V. J. (1993) Gradient tailored water suppression for $^{1}H-^{15}N$ HSQC experiments optimized to retain full sensitivity, *J. Magn. Reson., Ser. A 102*, 241−245.
34. Crippen, G. M., and Havel, T. F. (1988) *Distance Geometry and Molecular Conformation*, Research Studies Press, Somerset, England, and John Wiley, New York
35. Nilges, M., Clore, G. M., and Gronenborn, A. M. (1988) Determination of three-dimensional structures of proteins from interproton distance data by dynamical simulated annealing from a random array of atoms. Circumventing problems associated with folding, *FEBS Lett. 239*, 129−136.

36. Laskowski, R. A., MacArthur, M. W., Moss D. S., and Thornton J. M. (1993) Procheck: a program to check the stereochemical quality of protein structures, *J. Appl. Crystallogr. 26*, 283−291.
37. Koradi, R., Billeter, M., and Wüthrich, K. (1996) MOLMOL: a program for display and analysis of macromolecular structures, *J. Mol. Graphics 14*, 29−32.
38. Wada, K., Ozaki, Y., Matsubara, H., and Yoshizumi, H. J. (1982) Studies on purothionin by chemical modifications, *J. Biochem. 91*, 257−263.
39. Chau, M. H., and Nelson, J. W. (1992) Cooperative disulfide bond formation in apamin, *Biochemistry 31*, 4445−4450.
40. Price-Carter, M., Gray, W. R., and Goldenberg, D. P. (1996) Folding of $\omega$-conotoxins. 1. Efficient disulfide-coupled folding of mature sequences in vitro, *Biochemistry 35*, 15537−15546.
41. States, D. J., Dobson, C. M., and Creighton, T. E. (1980) A conformational isomer of bovine pancreatic trypsin inhibitor produced by refolding, *Nature 286*, 630−632.
42. Spear, M. A., Breakefield, X. O., Beltzer, J., Schuback, D., Weissleder, R., Pardo, F. S., and Ladner, R. (2001) Isolation, characterization, and recovery of small peptide phage display epitopes selected against viable malignant glioma cells, *Cancer Gene Ther. 8*, 506−511.
43. Christmann, A., Wentzel, A., Meyer, C., Meyers, G., and Kolmar, H. (2001) Epitope mapping and affinity purification of monospecific antibodies by escherichia coli cell surface display of gene-derived random peptide libraries, *J. Immunol. Methods 257*, 163−173.

BI020628H